"HARMONIE 37h1 radiation sensitivity tests" Supplement 3: Comparison of SBDART LOWTRAN and Kato HITRAN calculations

Kristian P. Nielsen [1], Emily Gleeson [2] & Laura Rontu [3]

1. Danish Meteorological Institute, Lyngbyvej 100, DK-2100, Copenhagen Ø, Denmark.

2. Met Éireann, Glasnevin Hill, Dublin 9, Ireland.

3. Finnish Metorological Institute, Erik Palménin Aukio 1, FI-00560 Helsinki, Finland.

In our initially submitted manuscript (Nielsen et al. 2013) we used the SBDART pseudo-spectral calculations (Ricchiazzi et al. 1998) that are based on the LOWTRAN 7 atmospheric transmission code of Pierluissi and Peng (1985). Referee #1 (Anonymous 2014) pointed out that we should rather use the more accurate correlated-k band parameterization made by Kato et al. (1999), which in libRadtran can be run with absorption coefficients calculated from the HITRAN 2000 database.

In this supplement a comparison is made between the results obtained when using the SBDART/LOWTRAN transmissions and the new results calculated using the Kato et al./HITRAN 2000 transmissions. For the clear sky experiments (Figs. 1–3 and 13–15) differences of a 0% to 2% increase in the simulated global radiation and net shortwave fluxes are found. For the cloudy sky experiments (Figs. 4–12 and 16–28) the differences are smaller. Overall using the Kato et al./HITRAN 2000 transmissions gives us more accurate results for testing the shortwave sensitivity of the HARMONIE NWP model, but the differences between running with these and the SBDART/LOWTRAN transmissions are too small to affect the main conclusions in our submitted manuscript. These results are of interest also for other studies that have used SBDART.

For further information about the experiments and results presented here please consult the original manuscript (Nielsen et al. 2013) and the references in this. The only change relative to this, is that the experiments have been rerun for the full shortwave spectral range rather than the interval from 280 nm to 3001 nm.

References

[1] Kato, S., Ackerman, T. P., Mather, J. H., and Clothiaux, E.: The k-distribution method and correlated-k approximation for a shortwave radiative transfer model, J. Quant. Spec. Rad. Transfer, 62, 109–121, 1999.

[2] Nielsen, K. P., Gleeson, E. and Rontu L.: Radiation sensitivity tests of the HARMONIE 37h1 NWP model, Geosci. Model Dev. Discuss., 6, 6775-6834, www.geosci-model-dev-discuss.net/6/6775/2013/doi:10.5194/gmdd-6-6775-2013, 2013.

[3] Pierluissi, J. H. and Peng, G.-S.: New molecular transmission band models for LOWTRAN, Opt. Eng., 24, 541–547, 1985.

[4] Anonymous referee #1: Review of "Radiation sensitivity tests of the HARMONIE 37h1 NWP model," Geosci. Model Dev. Discuss., 6, C2479C2483, www.geosci-model-dev-discuss.net/6/C2479/2014/, 2014.

[5] Ricchiazzi, P., Yang, S., Gautier, C. and Sowle D.: SBDART: A Research and Teaching Software Tool for Plane–Parallel Radiative Transfer in the Earth's Atmosphere, Bull. Am. Meteor. Soc., 79 (10), 2101–2114, 1998.
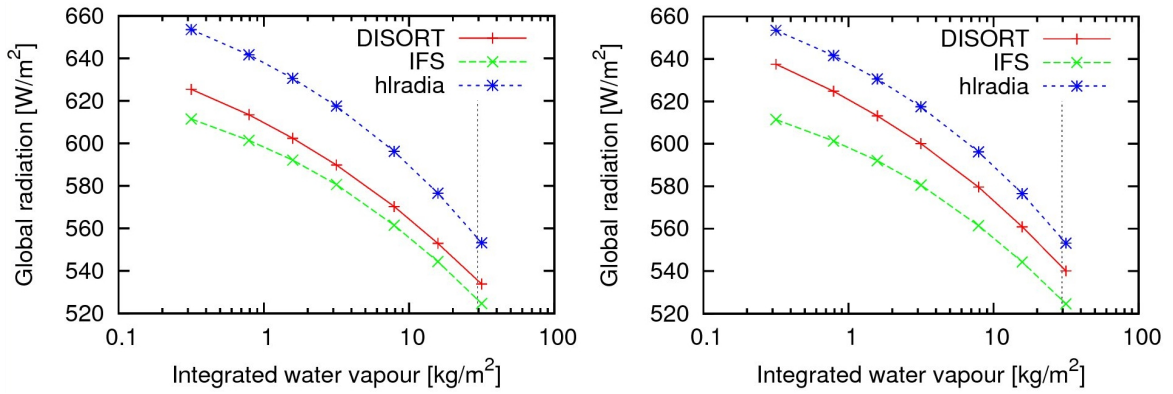
Figure 1: Comparison of global radiation results as a function of integrated atmospheric water vapour. The results from DISORT (red line with +), IFS (green line with x) and hlradia (blue line with *) are shown. The vertical dashed line marks the reference integrated water vapour used in the other experiments. **Left:** The results in the orginally submitted manuscript where the SBDART correlated-k distrubtion based on the LOWTRAN database was used as input to DISORT. **Right:** The recalculated results where the Kato correlated-k distrubtion based on the HITRAN 2000 database is used as input to DISORT.
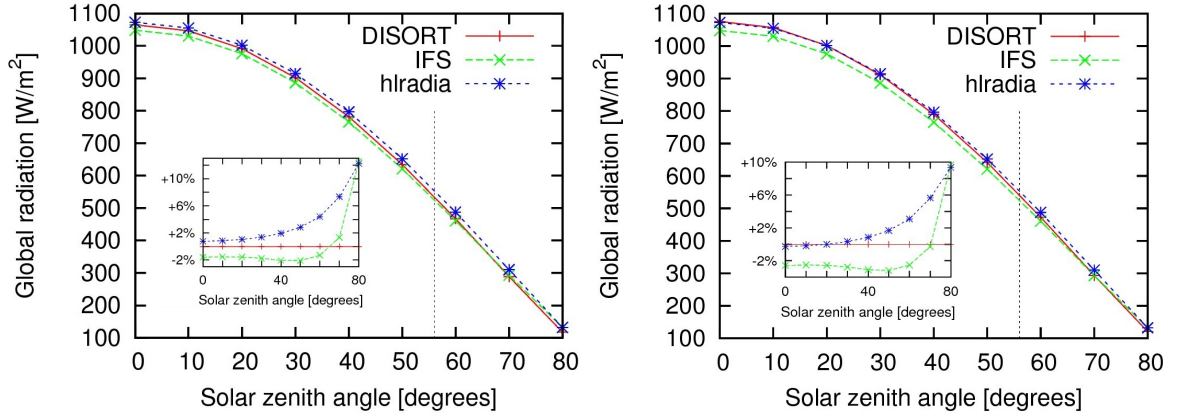
Figure 2: As for Fig. 1 but for a varying solar zenith angle. The subplots show the corresponding relative differences defined as (X-DISORT)/DISORT·100%.
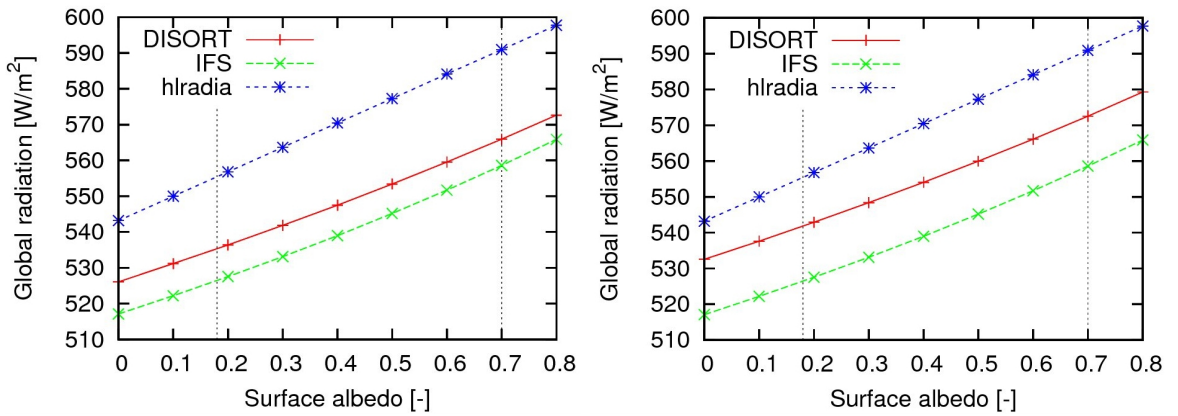
Figure 3: As for Fig. 1 but for a varying surface albedo in clear sky conditions.
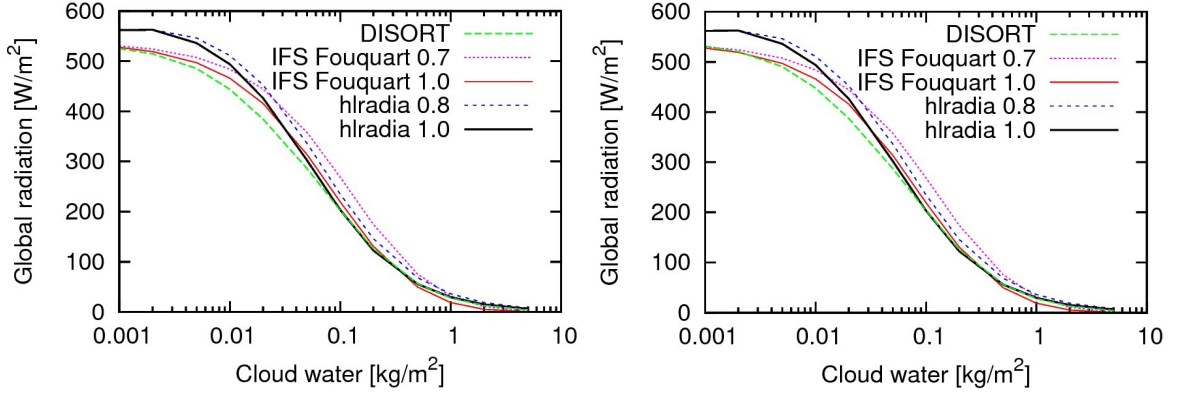
Figure 4: Comparison of global radiation results as a function of integrated liquid cloud water. The results from DISORT (green dashed curve), IFS Fouquart with SW inhomogeneity factors of 0.7 (magenta dotted curve) and 1.0 (red curve), and hlradia with SW inhomogeneity factors of 0.8 (blue dashed curve) and 1.0 (black curve) are shown. **Left:** The results in the orginally submitted manuscript where the SBDART correlated-k distrubtion based on the LOWTRAN database was used as input to DIS-ORT. **Right:** The recalculated results where the Kato correlated-k distrubution based on the HITRAN 2000 database is used as input to DISORT.
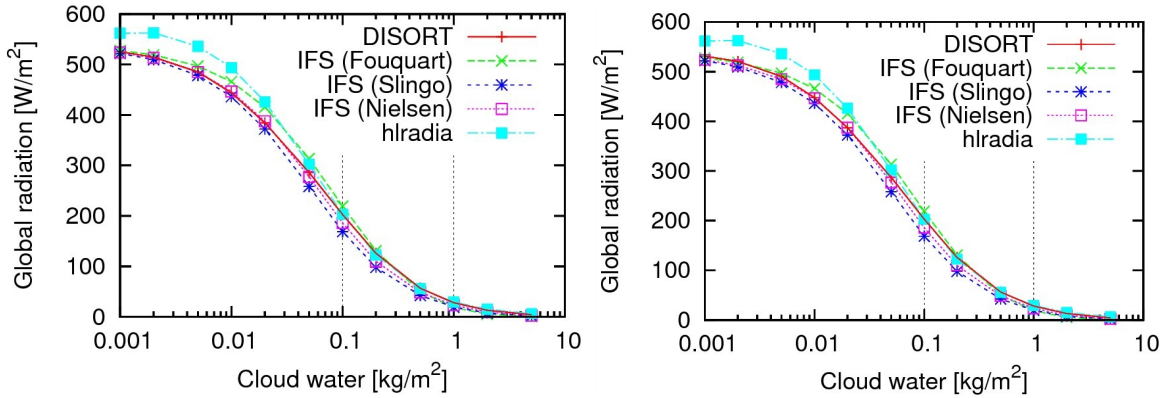
Figure 5: As for Fig. 4 but here the SW inhomogeneity factor is 1.0 in all cases. The results for DISORT (red curve with +s), IFS Fouquart (green curve with xs), IFS Slingo (blue curve with *s), IFS Nielsen (magenta curve with boxes) and hlradia (cyan curve with filled boxes) are shown.
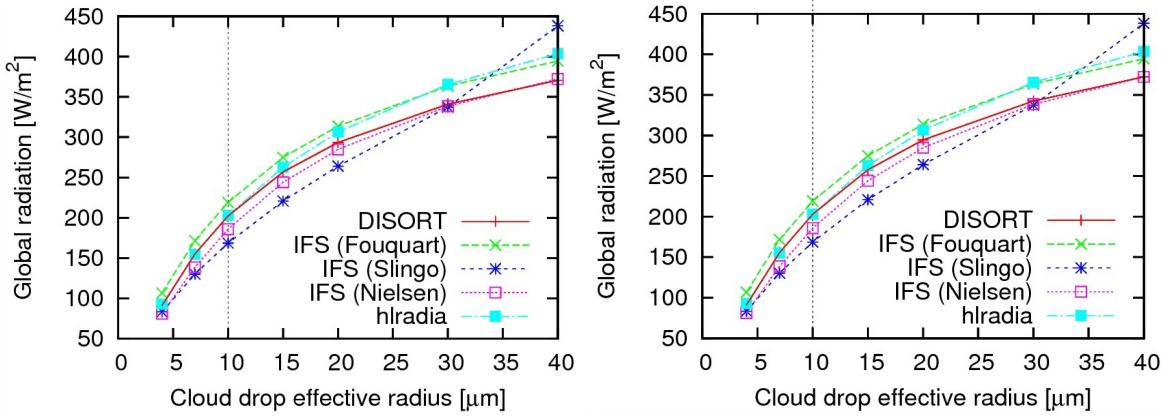
Figure 6: As for Fig. 5 but for a varying cloud drop effective radius.
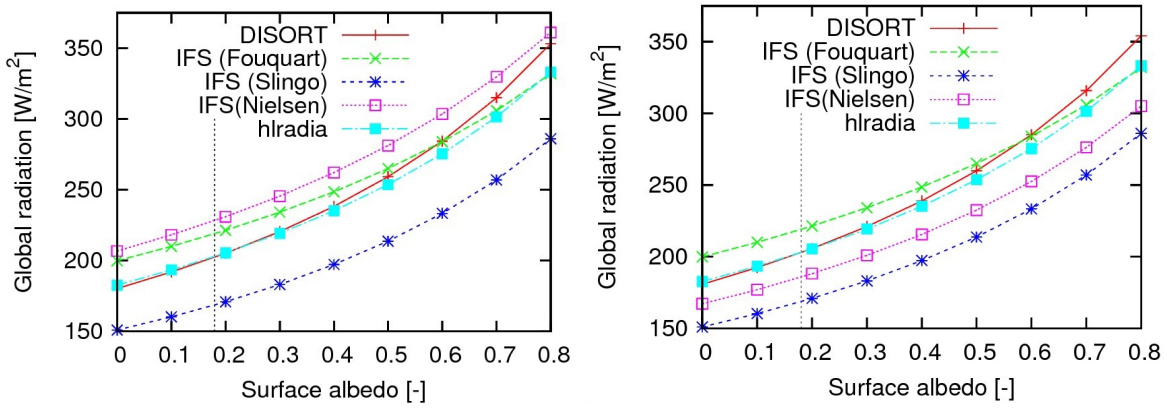
Figure 7: As for Fig. 5 but for a varying surface albedo under a cloud with 0.1 kg/m^2 cloud liquid water.
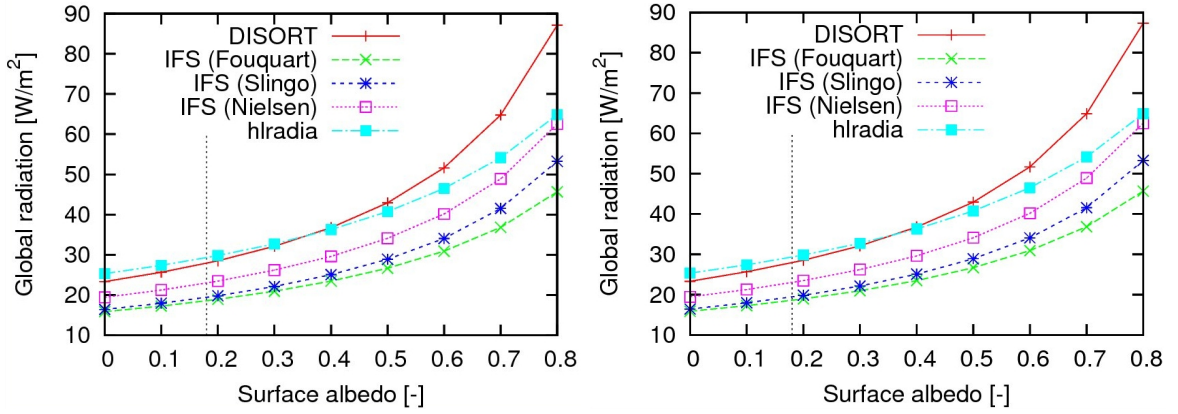
Figure 8: As for Fig. 5 but for a varying surface albedo under a cloud with 1.0 kg/m^2 cloud liquid water.
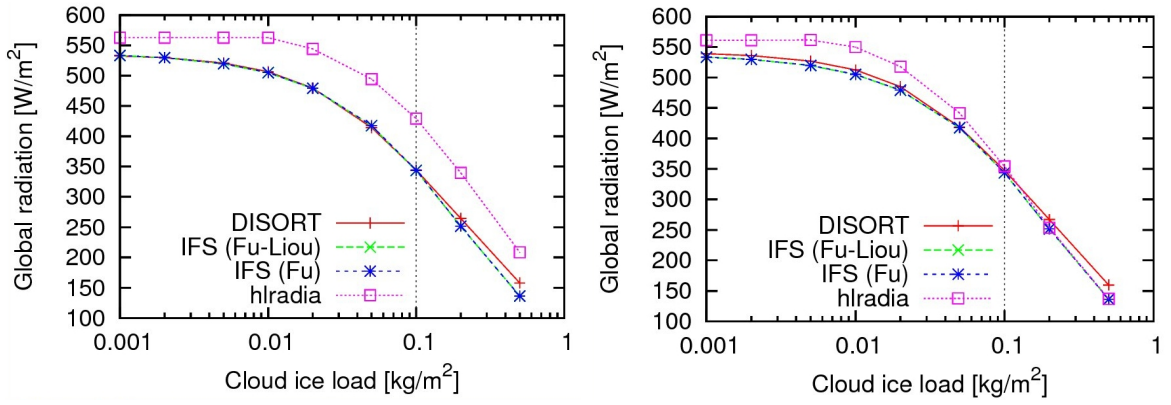
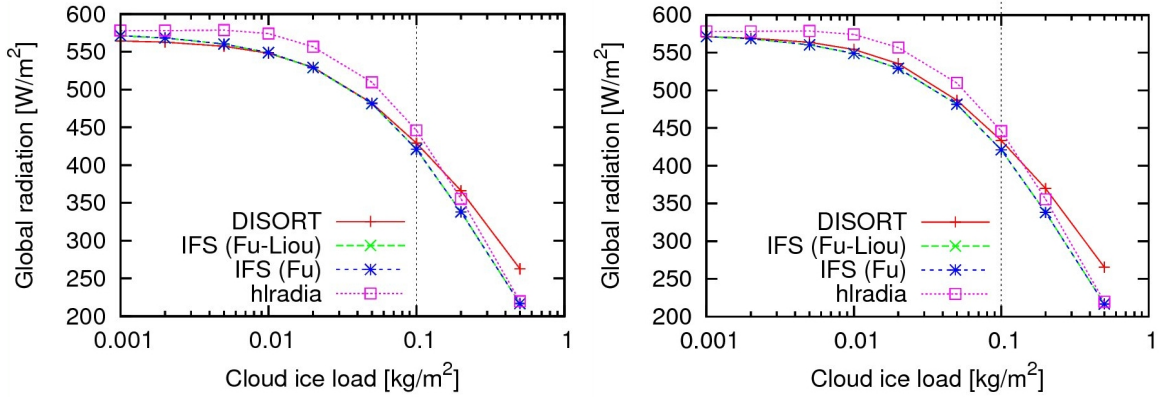Figure 9: As for Fig. 5 but for a varying cloud ice load.
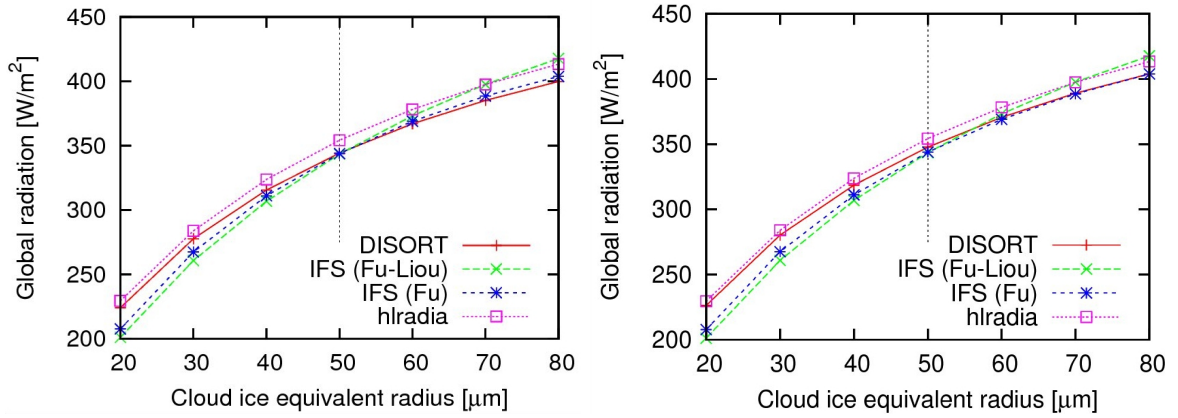
Figure 10: As for Fig. 9 but for surface albedo = 0.7.
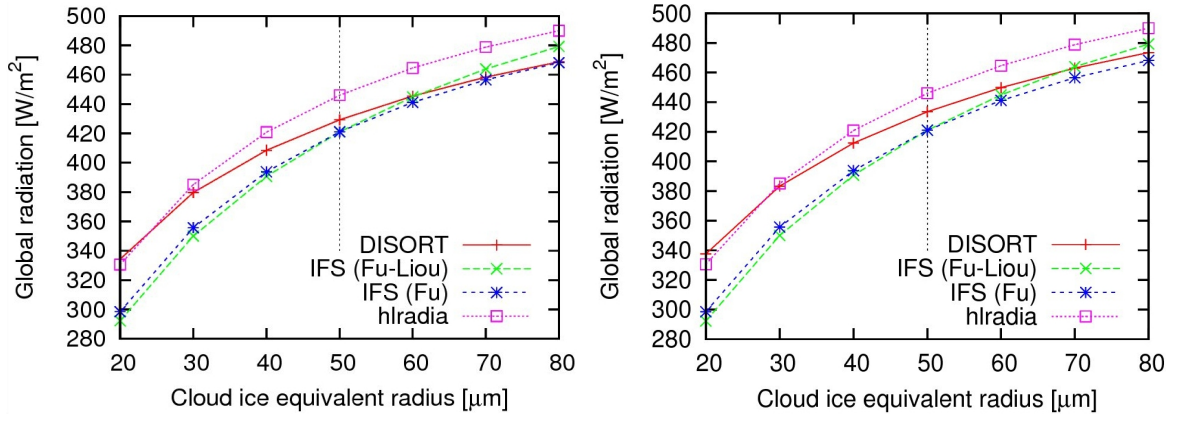

Figure 11: As for Fig. 5 but for a varying cloud ice equivalent radius.

Figure 12: As for Fig. 11 but for surface albedo = 0.7.
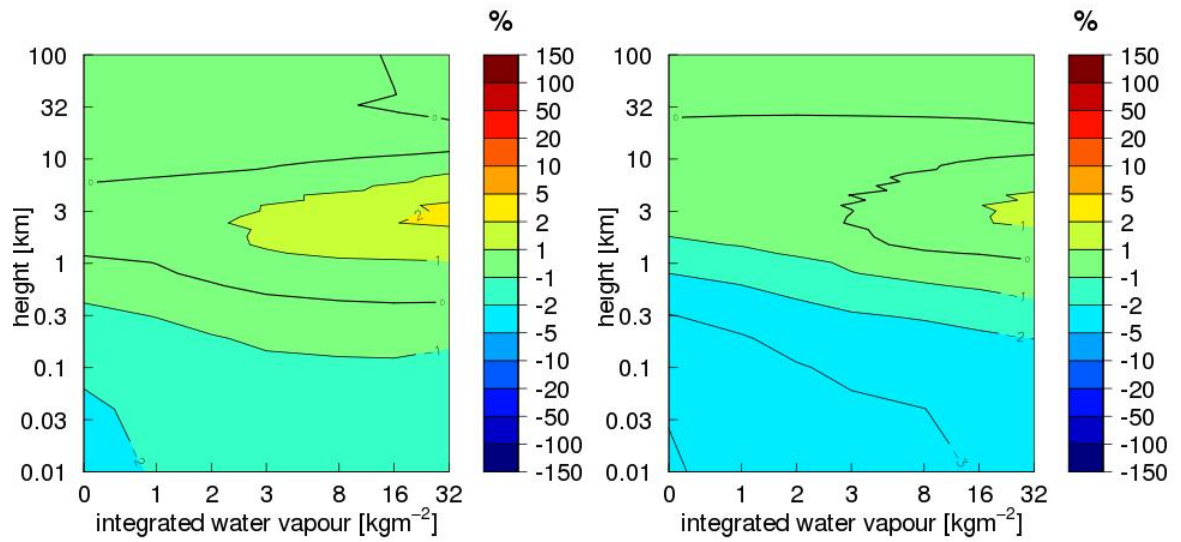
Figure 13: Relative differences (%) in net fluxes between the IFS radiation scheme and DISORT shown as a function of integrated water vapour and height.
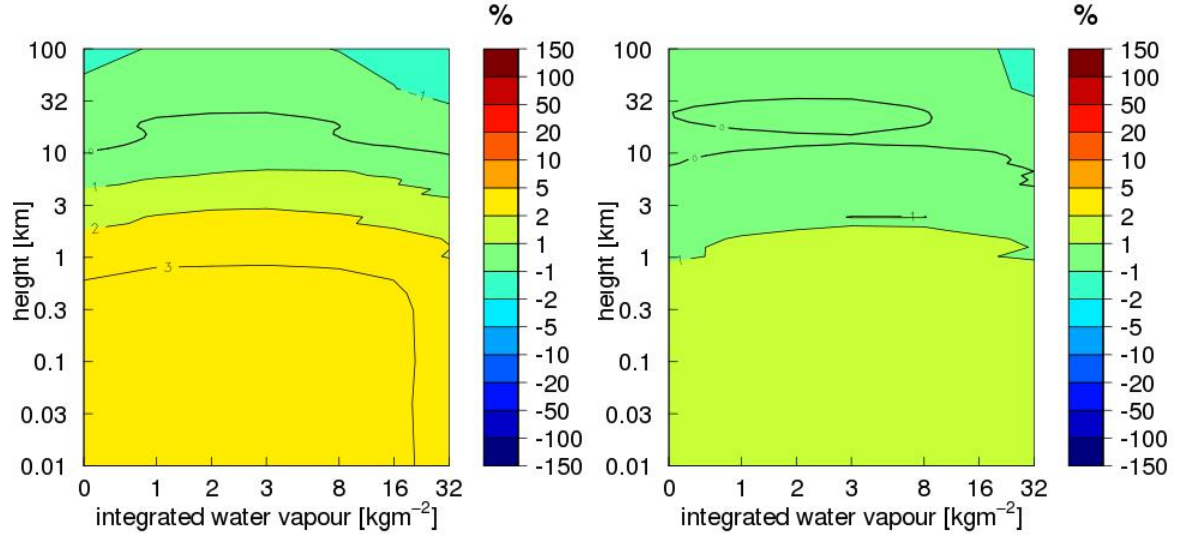
Figure 14: As for Fig. 13 but for hlradia compared to DISORT.
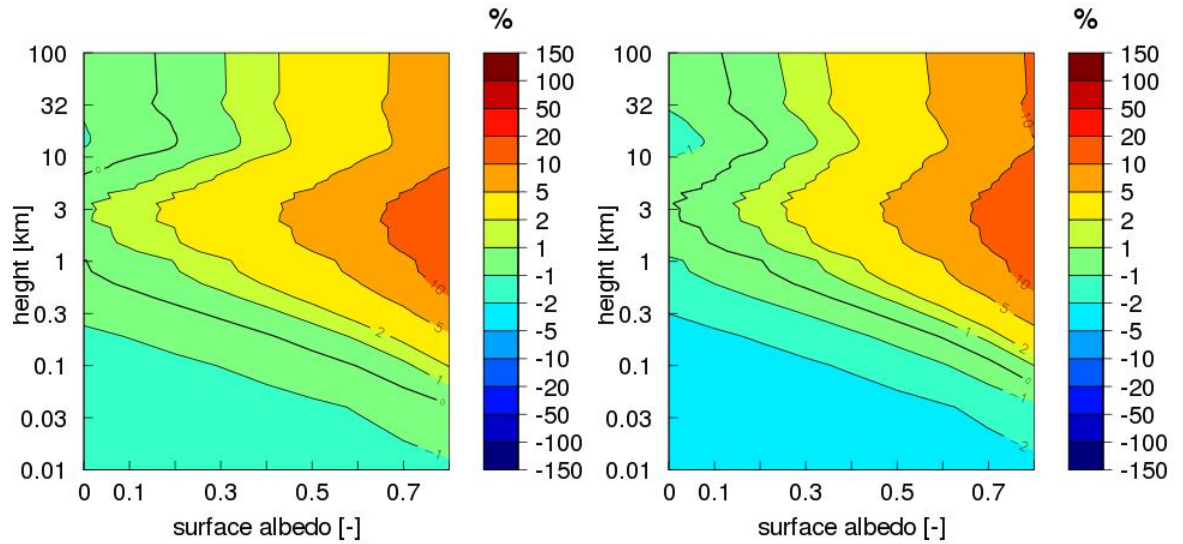
Figure 15: As for Fig. 13 but for IFS vs DISORT as a function of surface albedo.
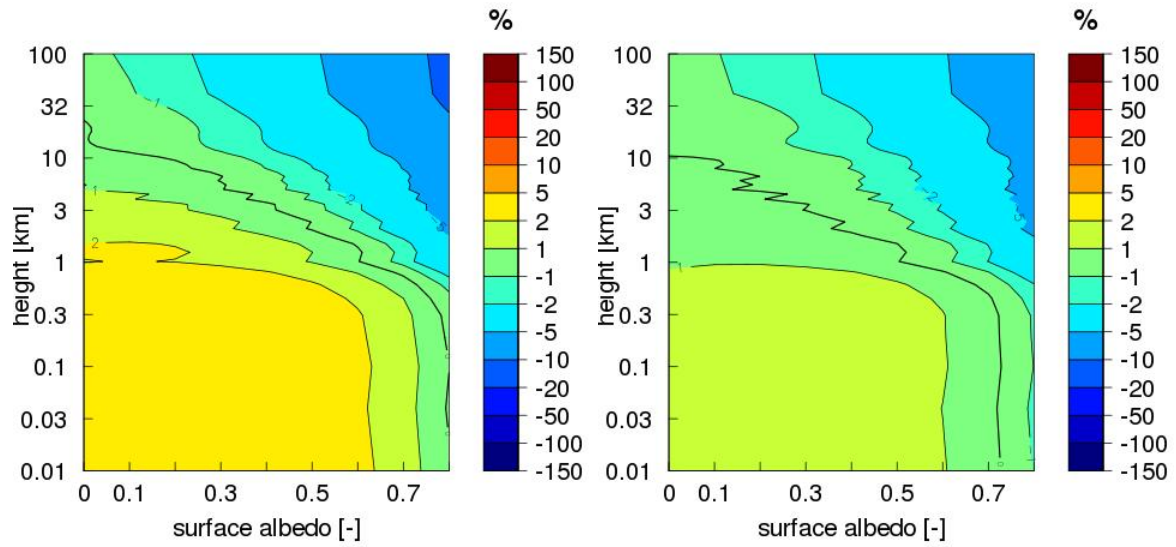
Figure 16: As for Fig. 15 but for hlradia compared to DISORT.
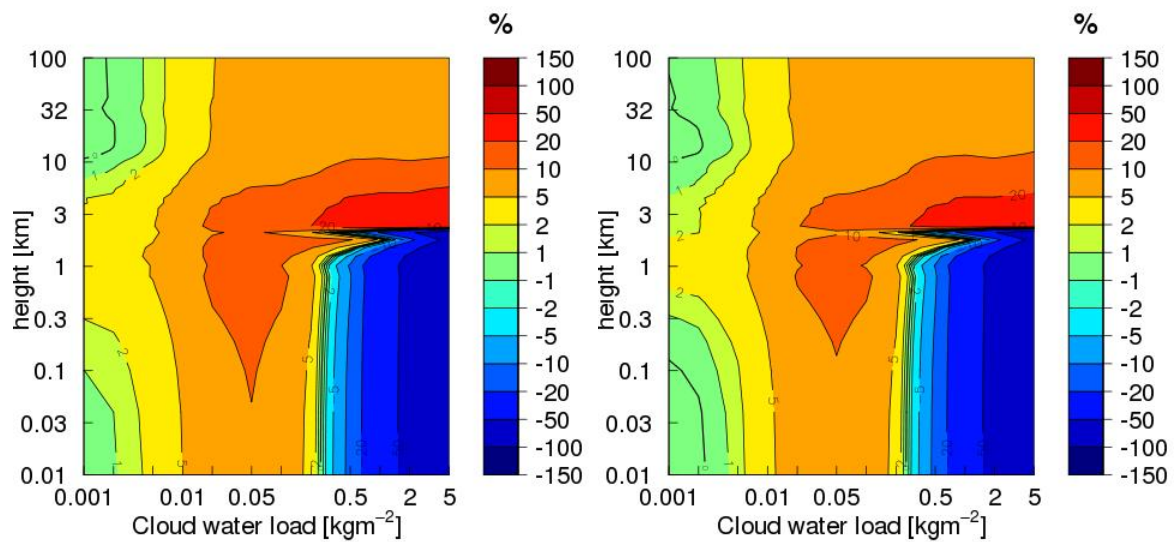
Figure 17: As for Fig. 13 but for cloud water load and IFS-Fouquart vs DISORT
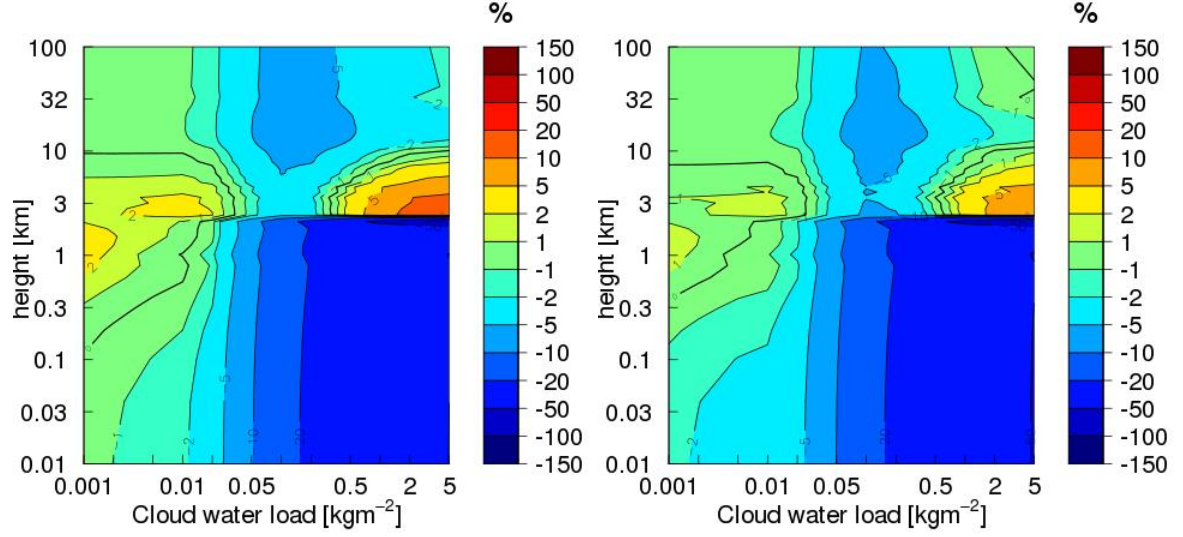
Figure 18: As for Fig. 17 but for IFS-Slingo vs DISORT.
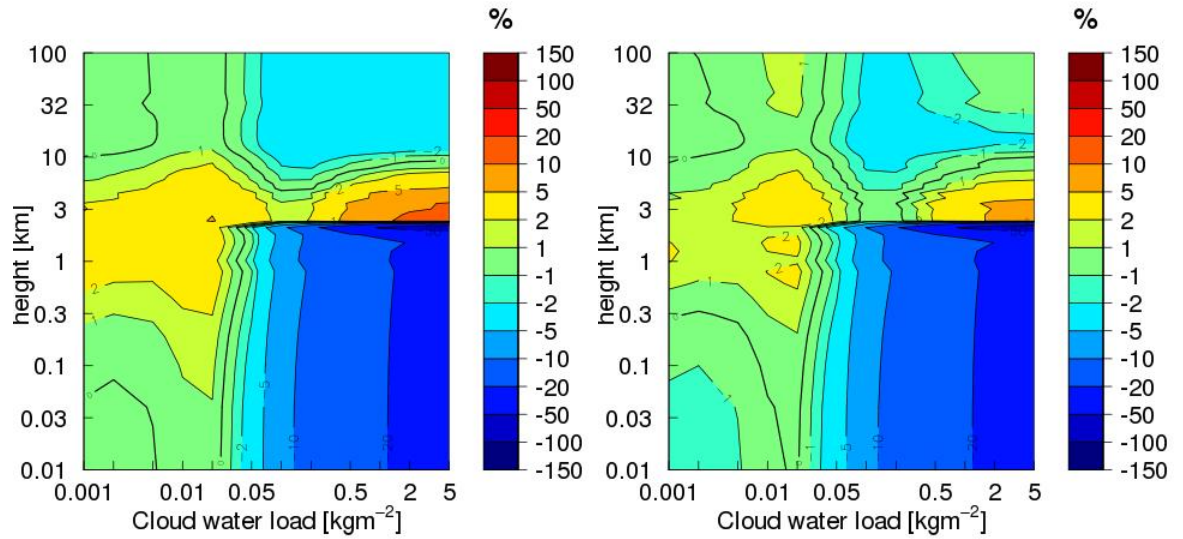
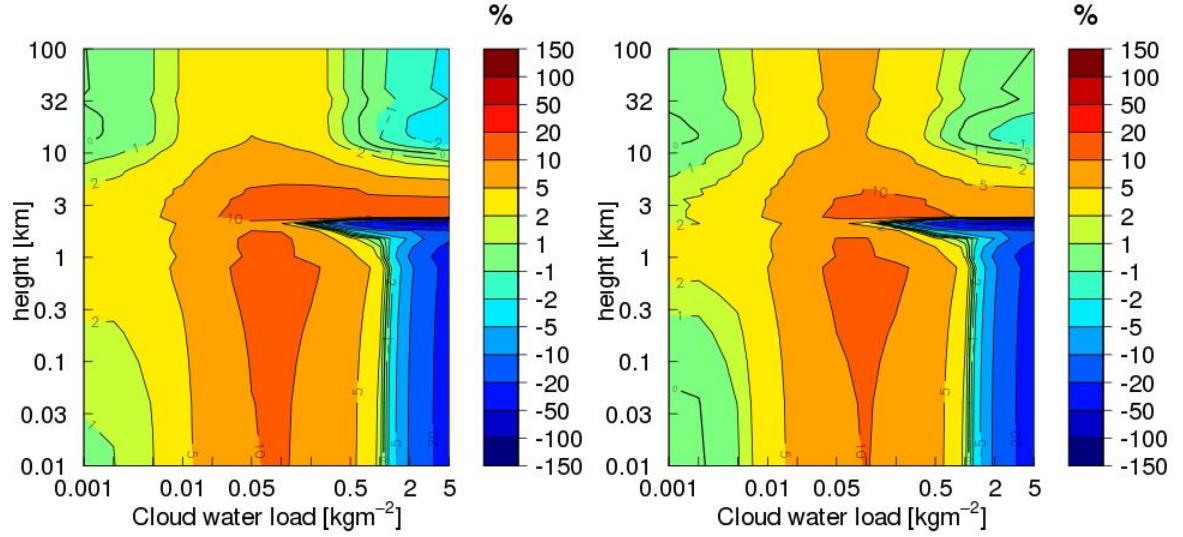

Figure 19: As for Fig. 17 but for IFS-Nielsen vs DISORT.

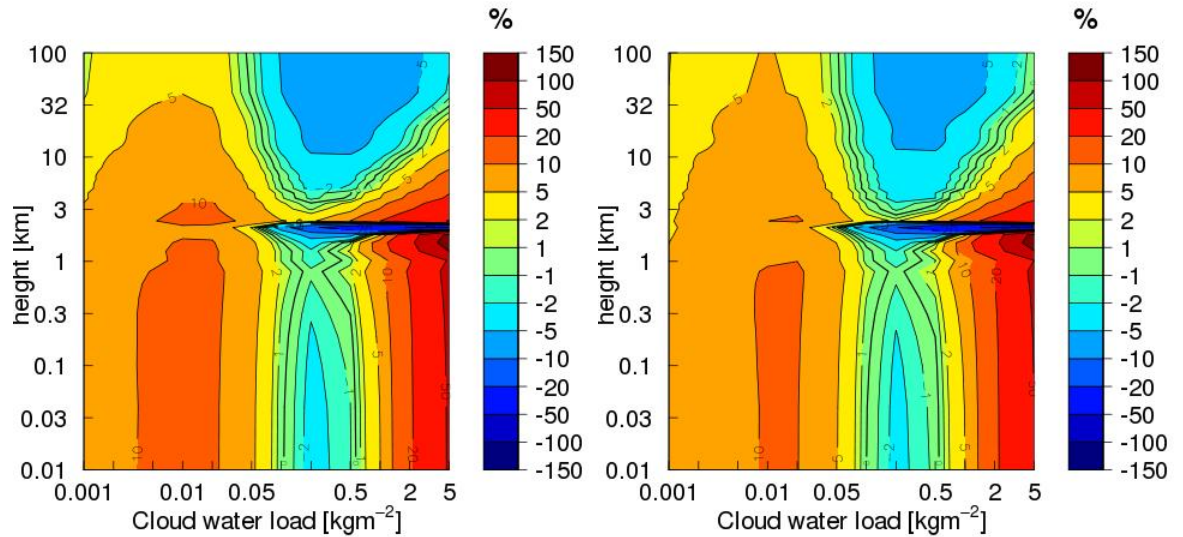Figure 20: As for Fig. 19 but for IFS-Nielsen with the Hopf q-function set to 0.71 vs DISORT.
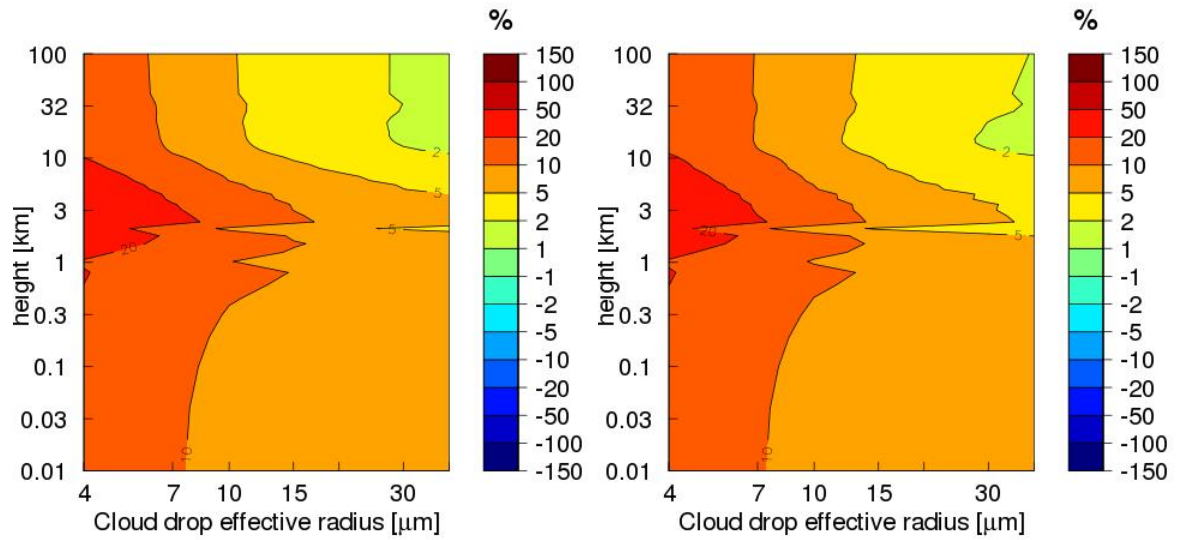

Figure 21: As for Fig. 17 but for hlradia vs DISORT.

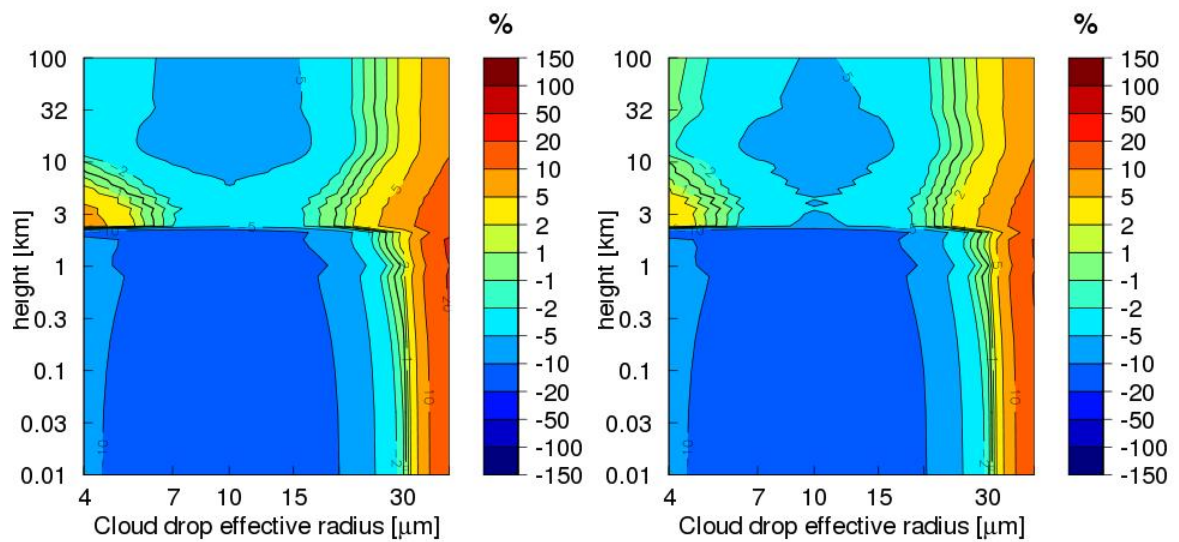Figure 22: As for Fig. 13 but for cloud drop effective radius and IFS-Fouquart vs DISORT

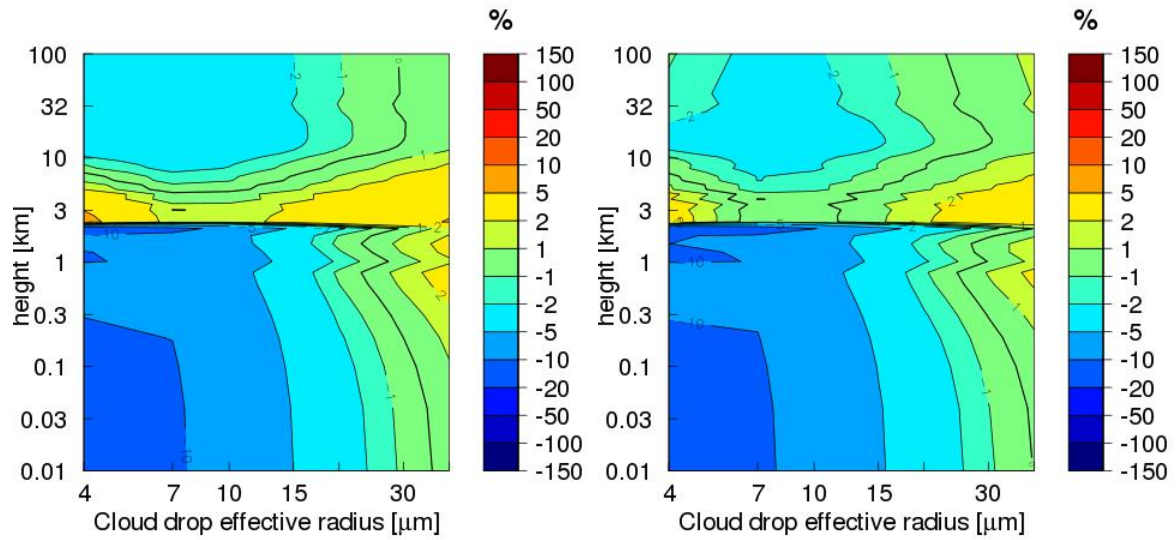Figure 23: As for Fig. 22 but for IFS-Slingo vs DISORT.

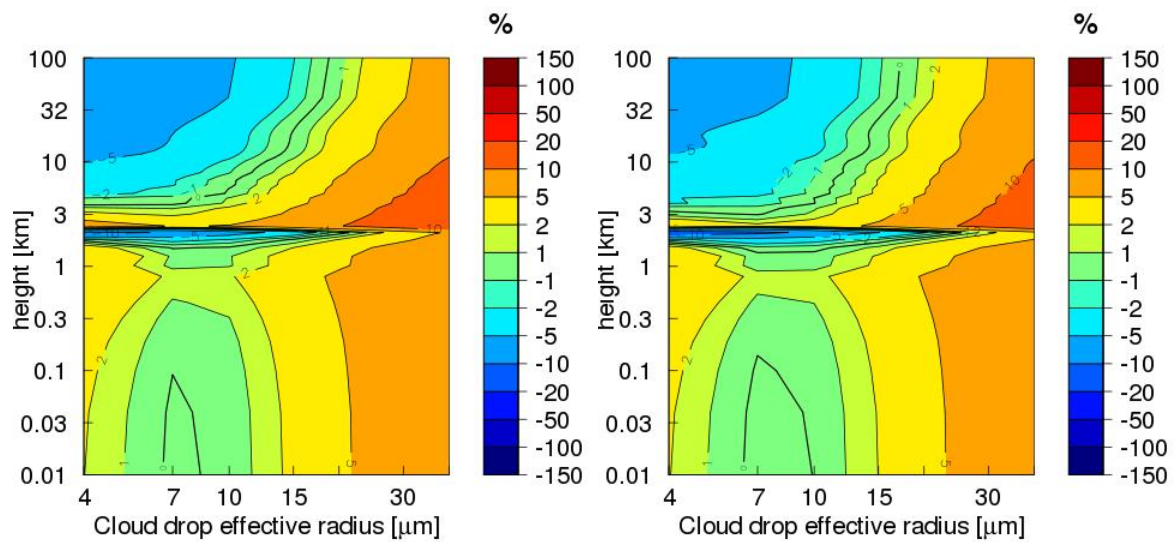Figure 24: As for Fig. 22 but for IFS-Nielsen vs DISORT.

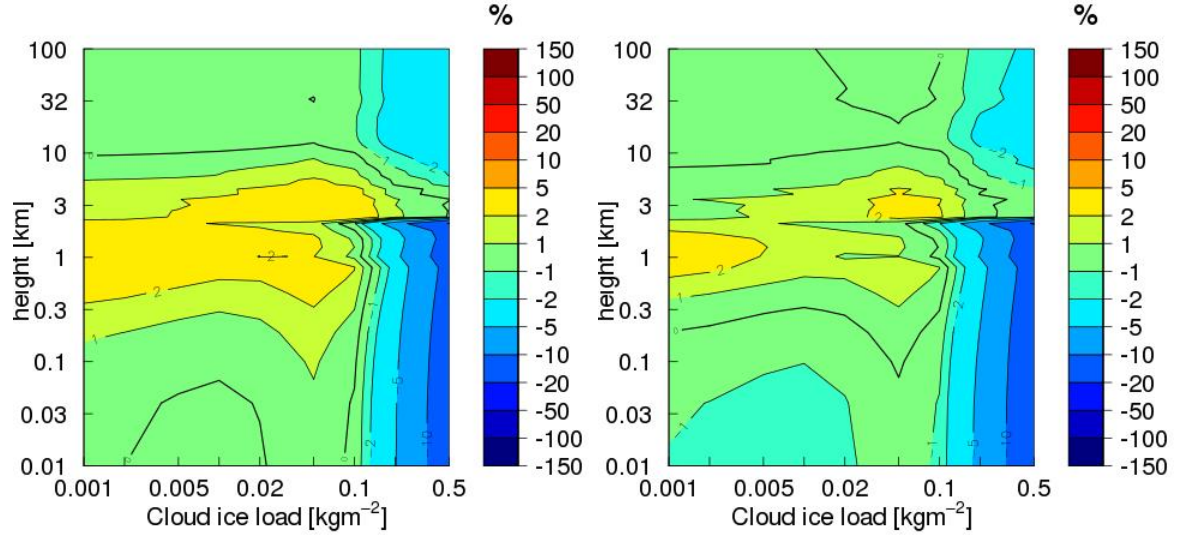Figure 25: As for Fig. 22 but for hlradia vs DISORT.

Figure 26: As for Fig. 13 but for cloud ice load and the IFS radiation scheme using the Fu and Liou (1993) ice cloud optical property parametrization vs DISORT.
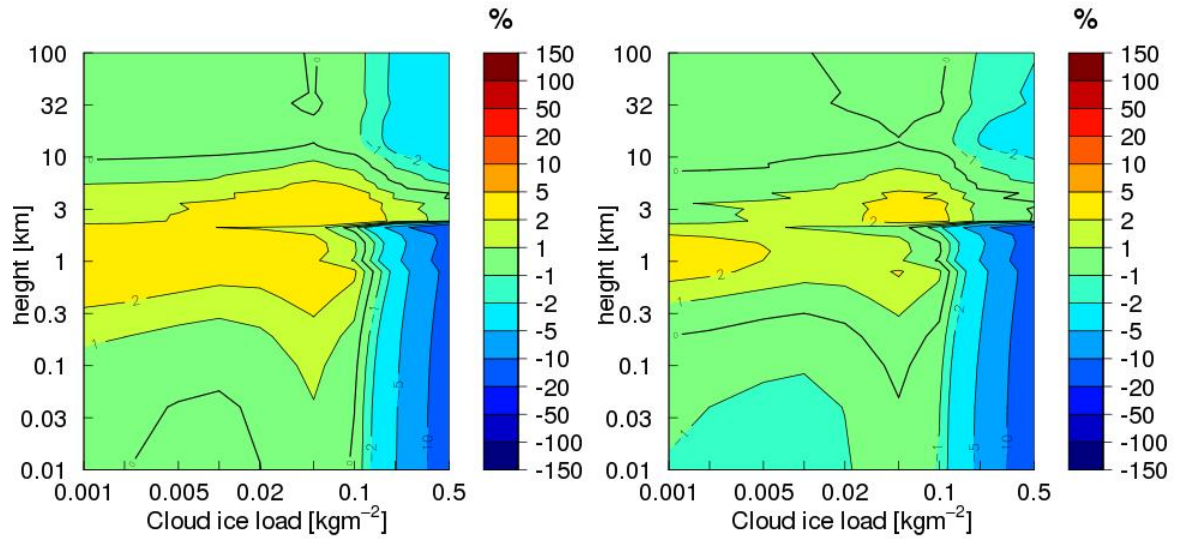

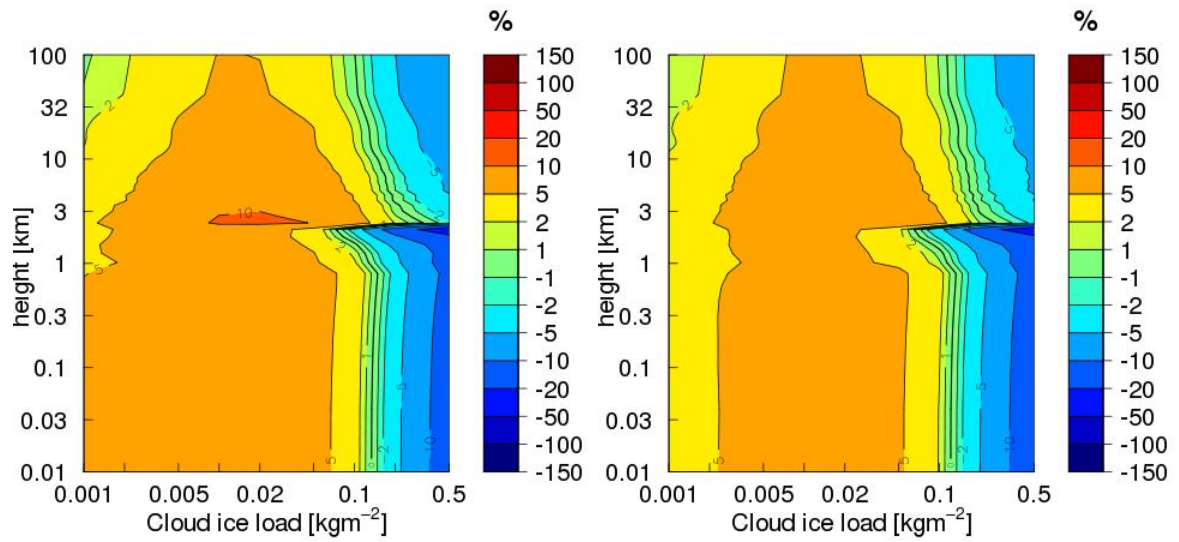Figure 27: As for Fig. 26 but for IFS with the Fu (1996) ice cloud optical property scheme vs DISORT.

Figure 28: As for Fig. 26 but for hlradia vs DISORT.